

A Structural Causal Model for Electronic Device Reliability: From Effects to Counterfactuals

Federico Mattia Stefanini

Department of Environmental Science and Policy, University of Milan,
Via Celoria 2, 20133 Milan, Italy
federico.stefanini@unimi.it

Nedka Dechkova Nikiforova

Department of Statistics Computer Science Applications "G. Parenti",
University of Florence, viale Morgagni 59, Florence, 50134 Florence, Italy
n.nikiforova@unifi.it

and

Rossella Berni*

Department of Statistics Computer Science Applications "G. Parenti",
University of Florence, viale Morgagni 59, Florence, 50134 Florence, Italy
rossella.berni@unifi.it

June 24, 2025

Abstract

Electronic devices exhibit changes in electrical resistance over time at varying rates, depending on the configuration of certain components. Since measuring overall electrical resistance requires partial disassembly, only a limited number of measurements are performed over thousands of operating hours. This leads to censored failure times, whether under natural stress or under accelerated stress conditions. To address these challenges, including device-specific failure thresholds, a parametric structural causal model is developed to extract information from both observational and experimental data, with the aim of estimating causal effects and counterfactuals, regardless of the applied stress regime. Synthetic data are used to illustrate the main findings.

Keywords: Bayesian inference, degradation models, causal estimand, observational study, experimental design, survival function

*The authors gratefully acknowledge the financial support from the Italian Ministry of University and Research (MUR) under the Project of Relevant National Interest (PRIN 2022), project code E3DM - CUP master:B53C24006390006; CUP: B53C24006400006.

1 Introduction

The estimate of reliability (Meeker et al. 2021) (Singpurwalla 2006) can be expensive and time-consuming, especially when dealing with electronic devices that are designed to be highly reliable. Modern reliability assessments combine information from multiple sources rather than relying solely on test data (Hund & Schroeder 2020). Observational data may come from end users, thus the analyst has no control over the data-collection process. The consequent biases that affect reliability estimates include: (i) selection bias if the available data are not representative of the target population because the data-collection process favors certain types of devices or operating conditions; (ii) confounding bias when omitted variables in the statistical model affect both the attribute under investigation and the response variable, confounding the relationship between them.

In this study, we consider the electrical resistance of electronic devices, focusing on factors such as surface finish, component type, and pin size. To measure the electrical resistance of a device, the machine in which it is installed must be partially disassembled, thus, besides the initial measurement at the beginning of the work in production, only three to five measurements of electrical resistance are typically performed over a time window of several thousand working hours. Measurement times are also well spaced apart in randomized experiments performed in controlled conditions to study the effect of one or more experimental factors, like the surface finish and the size of pins. Interval and right censoring follow in these cases because the exact failure time at which the electrical resistance increases over the defined threshold is not available. It is worth noting that even basic designed experiments are often performed under an accelerated stress regime, thus statistical models that assimilate data coming from different sources must also accommodate alternative regimes.

Most of the peculiar features of the above-described context may be faced by developing a causal model able to extract information from observational as well as experimental data. Different approaches to build a causal model have been developed in the last thirty years (Berzuini et al. 2012), thus we do not provide an exhaustive review of the topic. Dominici et al. (2021) and Brand et al. (2023) are two recent review papers in this field, including machine learning methods in causal inference. More precisely, Brand et al. (2023) deal with theoretical and terminological aspects, as well as with applications strictly related to the sociological field. Dominici et al. (2021) provide a detailed review of the potential outcomes framework for causal inference, explicitly considering the advantages and disadvantages of machine learning approaches to causal inference; moreover, the authors highlight open problems that remain unaddressed by current machine learning techniques. In Brand et al. (2023), a more comprehensive overview of the different approaches for causal inference is provided, with particular attention to path analysis and structural equation modeling in the sociological field. More specific review papers are provided by Degtiar & Rose (2023) and Vonk et al. (2023). To this end, Degtiar & Rose (2023) deal with methods for addressing external validity bias, by specifically concentrating on the approaches for generalizability and transportability. In Vonk et al. (2023), the most popular approaches in the causal inference literature are described, starting from the set of assumptions they rest on, and classified according to Pearl’s Causal Hierarchy, i.e., seeing-doing-imagining, (Bareinboim et al. 2022).

Structural Causal Models (SCMs, Pearl, 2009) are adopted here as the working framework because, in our context, they offer a cognitively appealing way to define direct causal relationships through deterministic functions and to qualitatively represent the set of considered relationships using causal Directed Acyclic Graphs (DAGs). An introduction to

the structural causal modeling framework in reliability studies is provided by Hund & Schroeder (2020), who deal with causal modeling tools in the field of reliability assurance for biased data sources. The authors consider two types of bias, i.e., selection bias and confounding bias, also performing a sensitivity analysis. In Ruiz-Tagle et al. (2022), a novel probabilistic approach to counterfactual reasoning is introduced in the context of system safety. To this end, the authors propose a methodology specifically oriented toward system safety, employing Bayesian network models to evaluate counterfactual hypotheses.

In this work, we develop a SCM to investigate changes in electrical resistance as a function of electronic device configuration, relative humidity, and operating time (in kilohours). The proposed model provides Bayesian estimates such as the failure time of an electronic device and the counterfactual value of electrical resistance under a hypothetically different observation time. Section 2 describes the main features of the reliability context assumed in this study. Section 3 introduces the basic concepts of non-parametric SCMs and DAGs, and presents a simple context involving only one measurement time for electrical resistance testing. In Section 4, a parametric SCM for observational studies is presented, in which three measurement times are considered. The structural equations and the probability density functions (after marginalization) are defined and describe the submodel tailored for studies conducted under accelerated stress conditions. Section 5 introduces two synthetic datasets, one for each stress regime. The prior distributions on model parameters are then defined. In this section, the average difference in the increase of resistance under varying configurations is analyzed in the accelerated stress regime, and a reliability formula is proposed. The no-stress regime is then examined and the predictive distribution of the failure time under a given configuration of the electronic device is derived, together with useful counterfactuals. Section 6 provides final remarks and conclusions.

2 Assessing the electrical resistance of electronic devices

The electrical resistance $y_{0,j} \in (0, \infty)$, measured in ohms, is recorded for an electronic device j prior to the start of its operation, at time $w_{0,j} = 0$ kilohours (i.e., thousands of hours). In the following analysis, the index j is consistently used to denote devices (i.e., statistical units), and n indicates the sample size. Other indices, such as i and r , may refer to different objects depending on the specific formula or context in which they appear. At time $w_{1,j} > 0$, the electrical resistance $y_{1,j} \in (0, \infty)$ is measured again. The random variable $W_{f,j}$ refers to the (unknown) failure time of device j , with sample space $\Omega_{W_f} = (0, \infty)$: the failure occurs if the electrical resistance, measured in ohm, increases by 10%, thus reaching the value $1.1 y_{0,j}$.

The reliability function, $R(w_j | \xi) = 1 - F(w_j | \xi) = P[W_{f,j} > w_j | \xi]$ in context ξ , also known as survival function, describes the probability that a device is still operational at time w_j . By substitution, we obtain:

$$P[W_{f,j} > w_j | \xi] = P[Y_{1,j} < 1.1 \cdot y_{0,j} | W_{1,j} = w_j, y_{0,j}] \quad (1)$$

where the electrical resistance $Y_{1,j}$ may depend on selected experimental factors besides the elapsed time $w_{1,j} = w_j$; some of them may also have an effect on the initial response $Y_{0,j}$.

Life-testing may be performed under different regimes (Singpurwalla 2006): (i) the regular no-stress (NS) condition where the electronic device works in standard conditions; (ii) the accelerated stress (AS) condition where the amount of stress acting on the tested electrical device is elevated. In our context, acceleration is performed by applying thermal

cycles where the temperature cyclically varies from 0 [C°] to 100 [C°] along time in controlled experiments. The AS regime is often adopted when the design of an experiment under the NS regime would entail a large amount of test time before yielding failures. Observational studies are typically performed under the NS regime. The regime variable A_j indicates whether on device j the AS regime, $A_j = a_2$, or the NS one, $A_j = a_1$, is in force.

Variables $W_{i,j}$, with $i = 1, 2, 3, \dots$ represent the subsequent measurement times for observation j , regardless of the operating regime (NS or AS), starting from the beginning of the study. The number of elapsed hours in the AS regime is naturally mapped into the number of thermal cycles performed.

In the following analysis, three experimental factors describing key characteristics of an electronic device are considered. For device j , the type of surface finish is indicated as $x_{S,j}$, and $\Omega_{x_S} = \{1, 2, \dots, n_S\}$ is the sampling space; the type of component is $x_{T,j}$, with $\Omega_{x_T} = \{1, 2, \dots, n_T\}$, while for the number of pins $x_{P,j}$ we have n_P levels, $\Omega_{x_P} = \{1, 2, \dots, n_P\}$. Following the literature, the change in electrical resistance of a device over time also depends on the humidity level during its operation. The relative humidity, $x_{H,j}$, is represented by n_H integers, each one corresponding to an interval in a partition defined over a scale ranging from 0% to 100%. In our context, the partition consists of two elements: the normal range, $x_H = -1$, and high range, $x_H = 1$.

3 Structural Causal Models and the minimal DAG

A Non-Parametric Structural Causal Model (NP-SCM, Pearl 2009, Definition 7.1.1, modified) is a triple $\mathcal{S} = \langle U, V, \mathcal{H} \rangle$, where $V = \{V_1, V_2, \dots, V_i, \dots\}$ is a finite collection of endogenous variables. Each variable $V_i \in V$ is explicitly related to other variables in V and in $U = \{U_1, U_2, \dots, U_i, \dots\}$, the finite set of exogenous-background variables. The exogenous variable U_i collects all other causal determinants of V_i not explicitly included in the model as endogenous variables. The set of deterministic functions $\mathcal{H} = \{h_1, h_2, \dots, h_i, \dots\}$ contains one function for each endogenous variable; for node V_i , the function $h_i()$ maps arguments $U_i \cup \{pa_i\}$ to the result V_i , therefore $V_i = h_i(pa_{i,1}, pa_{i,2}, \dots, U_i)$; the notation $pa_i = \{pa_{i,1}, pa_{i,2}, \dots\} \subset V \setminus V_i$ refers to the collection of endogenous variables entering as argument into h_i , and it is motivated by the qualitative representation of these mappings through the directed acyclic graphs described in this section. In the following analysis, we assume that the exogenous variables in U are marginally independent, thus, the joint distribution is:

$$p(u_1, u_2, \dots, u_r, \dots, u_{n_V}) = \prod_{r=1}^{n_V} p(u_r)$$

where $n_V = |V|$ is the total number of nodes. Our expert believes this is a reasonable assumption at the considered level of model granularity. In other terms, endogenous variables are explicitly and causally related, while exogenous variables incorporate all residual causal determinants. NP-SCMs are structural because (implicit) deterministic functions relate exogenous variables; they are modular because the intervention on a variable V_i implies a local change of the manipulated variable, i.e., its deterministic function h_i becomes equal to the constant assigned by intervention.

A DAG \mathcal{G} is defined by a triple $\mathcal{G} = \langle V, U, E \rangle$, and it qualitatively represents the causal relationships in a SCM (Pearl 2009). The nodes in the two sets V and U correspond to endogenous and exogenous variables respectively. The set E contains directed edges that join arguments in the deterministic function $h_i \in \mathcal{H}$, called parents $pa_i = \{pa_{i,1}, pa_{i,2}, \dots\}$, to the endogenous variable V_i . An oriented edge, say $X_S \rightarrow Y_1$, represents a direct causal

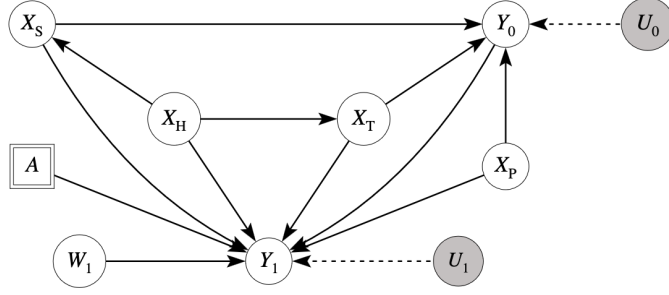


Figure 1: DAG \mathcal{G}_1 for the minimal observational study on a soldering process with regime indicator A and exogenous variables U_0, U_1 (grey background) acting on Y_0 and Y_1 made explicit.

relationship of X_S on Y_1 (e.g., Figure 1) at the considered level of model granularity. All endogenous variables are represented in a causal DAG, while (some) exogenous variables are often omitted unless they are essential at a particular stage of the analysis.

In Figure (1), the minimal causal DAG consisting of only one measurement time W_1 is decorated to improve the representation. Dashed arrows join exogenous to endogenous variables Y_0 and Y_1 , while solid lines always pertain endogenous-to-endogenous causal relationships. The grey background of U_0 and U_1 emphasizes that they are exogenous random variables, while all endogenous variables have white background to highlight that realizations depend on the value taken by all parent nodes according to the underlying deterministic functions. The regime variable A is located within a rectangle to make explicit that it is a known attribute, i.e., it is always known which regime is in force.

In the causal DAG \mathcal{G}_1 (Figure 1), the electrical resistance Y_1 measured at time W_1 depends on the initial electrical resistance Y_0 and on covariates X_S, X_T, X_P , besides humidity X_H . The level of humidity X_H also determines the probability that the electronic device is configured as (x_S, x_T) by the end user, e.g., a specific type of component and surface finish is favored when humidity is high. Variable X_H satisfies the back-door criterion (Pearl 2009, theorem 3.3.2), thus in this first simple observational study the causal effect of X_S on Y_1 conditional on w_1 is obtained as:

$$p(y_1 \mid do(x_S), w_1) = \sum_{x_H} p(y_1 \mid x_S, w_1, x_H) p(x_H)$$

where the estimand on the left is rewritten in terms of quantities available from an observational study: confounding bias is removed.

The counterfactual variable $Y_{1,j,w_1}(w')$ is defined as the value of electrical resistance that would have been measured at time $W_{1,j} = w'$ in the electronic component j , whereas the actual measurement was taken at time $W_{1,j} = w$, yielding the observed value $Y_{1,j} = y$. A common notation for counterfactual variables assigns a subscript to each manipulated variable. For example, $Y_{1,j,w_1}(w') = h_{Y,1}(y_{0,j}, x_{S,j}, x_{T,j}, x_{P,j}, x_{H,j}, w', a, u_{1,j})$, where $u_{1,j}$ denotes the realization of the exogenous variable $U_{1,j}$ in the factual (i.e., observed) world in which $W_{1,j} = w$ and $y_{1,j}$ are measured.

Twin networks (Pearl 2009, section 7.1.4) are DAGs representing factual and counterfactual worlds. In Figure 2, the background nodes shared between the factual and counterfactual worlds are not duplicated (Ruiz-Tagle et al. 2022). Therefore, only the nodes

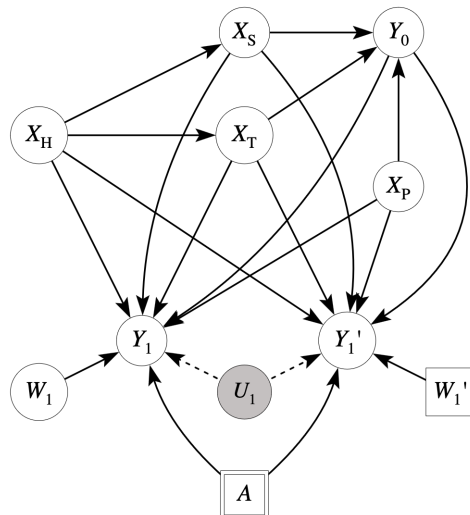


Figure 2: DAG \mathcal{G}_2 of the twin network (modified) based on \mathcal{G}_1 for what could have happened if W_1 in electronic device j had been equal to w' instead of the observed value w .

Y_1 and W_1 , which differ across worlds, are replicated in the counterfactual representation. This DAG shows the way to solve the question about the increase of electrical resistance due to a different amount of elapsed time in this simple context, but it may also be useful to answer the following question: which is the amount of target time $W_{1,j} = w''$ that I should have waited for the electronic device j in order to observe a value of electrical resistance equal to $1.1 \cdot y_{0,j}$, given that $y_{1,j}$ was observed at time w ? The answer is available if we can solve the deterministic equation that defines the failure time from the equality $Y_{1,j,w_1}(w'') - 1.1 \cdot y_{0,j} = 0$ given the endogenous parents in DAG \mathcal{G}_2 (Figure 2). We note in passing that $u_{1,j}$ is calculated in the factual world, using the observed value of $y_{1,j}$; furthermore, not only epistemic (knowledge-based) uncertainty but also aleatory uncertainty arising from the inherent randomness of a process cannot be neglected, especially in the case of limited sample sizes.

4 A parametric Structural Causal Model

In this section more details are provided about the considered context in which a total of four measurements are performed on each electronic device. The qualitative representation of the SCM elicited from the expert is shown in Figure (3), and it accommodates both observational studies under the NS regime and experiments in the AS regime, where four measurements are performed including $y_{0,j}$. The implicit deterministic functions in \mathcal{H} are now refined into parametric models, where the posterior distribution of unknown parameters given data is approximated by Markov Chain Monte Carlo (MCMC) simulation. All exogenous variables are here assumed to be marginally independent.

An observational study, in our context, is performed by gathering data from a sample of devices installed in production sites worldwide. Nodes X_S, X_T, X_P are categorical variables representing the configuration of the current electronic device j in terms of the selected features, while $X_H = h_H(U_H)$ indicates intervals of relative humidity. Our expert

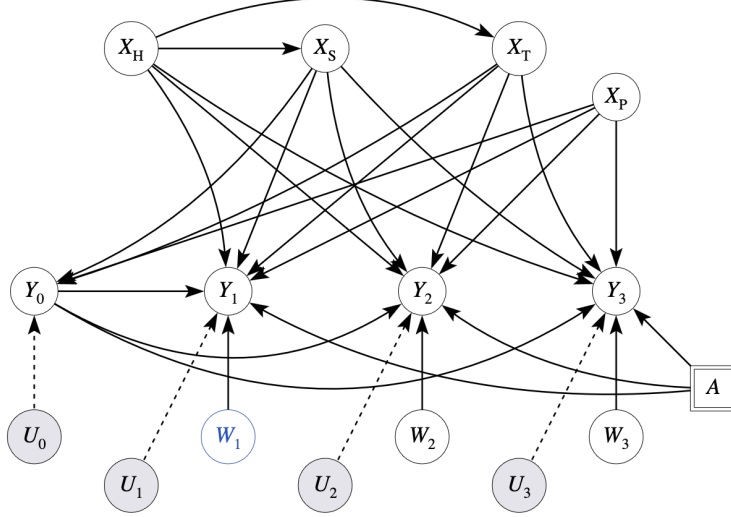


Figure 3: DAG \mathcal{G}_3 for observational studies with regime indicator A ; exogenous variables are included only when acting on the electrical resistance Y_i , $i = 0, 1, 2, 3$ of the electronic device.

believes that the configuration of each electronic device is selected by considering the typical humidity that occurs during operation in the assigned production site. If humidity is higher than 75% for 5 or more hours in a day then $X_H = +1$ indicates high relative humidity, otherwise $X_H = -1$ indicates normal relative humidity. After marginalization of the exogenous variable U_H , the induced binary random variable X_H is defined as:

$$p(x_H | \boldsymbol{\pi}_H) = \sum_{i \in \{-1, +1\}} \pi_{H,i} I_{(i)}(x_H) \quad (2a)$$

$$\Omega_{X_H} = \{-1, +1\} \quad (2b)$$

$$\pi_{H,+1} = 1 - \pi_{H,-1} \quad (2c)$$

with $I_{(i)}(x)$ the indicating function equal to 1 if $x = i$, zero otherwise. The number of pins is here modeled as a categorical variable after integrating out its exogenous variable U_P :

$$p(x_P | \boldsymbol{\pi}_P) = \sum_{i=1}^{n_P} \pi_{P,i} I_{(i)}(x_P) \quad (3a)$$

$$\Omega_{X_P} = \{1, 2, \dots, n_P\} \quad (3b)$$

$$\sum_{i=1}^{n_P} \pi_{P,i} = 1 \quad (3c)$$

where the notation parallels what defined for X_H .

The endogenous variables $X_S = h_S(x_H, U_S)$ and $X_T = h_T(x_H, U_T)$ receive an edge from X_H (Figure 3), and the induced random variables conditional on X_H are defined as follows:

$$p(x_S | \boldsymbol{\pi}_S, x_H = i) = \sum_{i=1}^{n_H} I_{(i)}(x_H) \sum_{r=1}^{n_S} \pi_{S,i,r} I_{(r)}(x_S) \quad (4a)$$

$$\Omega_{X_S} = \{1, 2, \dots, n_S\} \quad (4b)$$

$$\sum_{r=1}^{n_S} \pi_{S,i,r} = 1 \quad \forall i \in \{1, \dots, n_H\} \quad (4c)$$

$$p(x_T | \boldsymbol{\pi}_T, x_H = i) = \sum_{i=1}^{n_H} I_{(i)}(x_H) \sum_{r=1}^{n_T} \pi_{T,i,r} I_{(r)}(x_T) \quad (4d)$$

$$\Omega_{X_T} = \{1, 2, \dots, n_T\} \quad (4e)$$

$$\sum_{r=1}^{n_T} \pi_{T,i,r} = 1 \quad \forall i \in \{1, \dots, n_H\} \quad (4f)$$

thus matrices $\boldsymbol{\pi}_S$ and $\boldsymbol{\pi}_T$ have rows adding to one.

Two remarks are due, although already mentioned for the simple DAG of Section (3). First, Humidity X_H plays a special role working with observational data because it is a parent of nodes X_S, X_T and also a parent of the outcome Y_t , for all time points $t > 0$. In other words, X_H is a confounding variable in the estimate of the causal effects of X_S and X_T on Y_t at a specified value of time w_t . Second, the node A is represented by a double-rectangle to emphasize its nature of known regime indicator, i.e., a context variable without exogenous input. Edges $A \rightarrow Y_t$, with $t > 0$, make explicit the dependence of the electrical resistance on the adopted regime. In all observational studies $A = a_1$ because a NS regime is in force.

The measurement time since a device was turned on is represented by nodes W_1, W_2, W_3 if no more than three appointments are feasible in production. In Figure (3), variables W_1, W_2, W_3 are inside circular nodes because the exact time of measurement might be unrecorded, but for device j it is known that such value is close to the nominal value $\mu_{W,i}$. Therefore, the structural specification $W_{r,j} = h_r(U_{W,r,j})$, for $r \in \{1, 2, 3\}$, is refined into a parametric specification by quantifying the expert's uncertainty as follows:

$$\begin{aligned} w_{r,j} &= \mu_{W,r} + ((u_{W,r,j} - 1/2) * 1/100), \quad r \in \{1, 2, 3\} \\ U_{W,r,j} &\sim \text{Beta}(5, 5) \end{aligned} \quad (5)$$

thus a symmetric distribution is defined whose mode is $\mu_{W,r}$ ranging around the nominal value by five hours, i.e., $\mu_{W,r} \pm 0.005$. In our synthetic case study, we consider 30, 90, 150 days, thus $(\mu_{W,1}, \mu_{W,2}, \mu_{W,3}) = (0.72, 2.16, 3.60)$ kilohours.

The core component of our Bayesian SCM is a parametric model describing electrical resistance across four observation times. The equation $Y_0 = h_{Y_0}(x_S, x_P, x_T, U_0)$ takes the following parametric form:

$$y_{0,j} = \mu_0 + \sum_{r=1}^{n_S} \alpha_{S,r} I_{(r)}(x_{S,j}) + \sum_{r=1}^{n_T} \alpha_{T,r} I_{(r)}(x_{P,j}) + \sum_{r=1}^{n_P} \alpha_{P,r} I_{(r)}(x_{T,j}) + u_{0,j} \quad (6)$$

where μ_0 is the marginal mean and it is expected to be equal to the nominal value of electrical resistance for the considered devices (e.g., 1000 ohms). Given the sum-to-zero parameterization, alphas in equation (6) for the same endogenous variable add to zero, e.g., $\sum_{r=1}^{n_S} \alpha_{S,r} = 0$. The random variable $U_{0,j} \sim N(0, \sigma_0^2)$ represents the overall contribution of all causal determinants not accounted for as endogenous variables to the initial electrical

resistance Y_0 . As regards nodes Y_t with $t \in \{1, 2, 3\}$, the non-parametric specification $y_t = h_{Y_t}(y_0, x_S, x_P, x_T, x_H, w_t, a', u_t)$ is refined into the following parametric equation:

$$y_{t,j} = y_{0,j} + \quad (7a)$$

$$+ \left(\beta_1 + \sum_{r=1}^{n_S} \delta_{1,S,r} I_{(r)}(x_{S,j}) + \sum_{r=1}^{n_T} \delta_{1,T,r} I_{(r)}(x_{T,j}) + \sum_{r=1}^{n_P} \delta_{1,P,r} I_{(r)}(x_{P,j}) + \quad (7b)$$

$$+ \sum_{r=1}^{n_H} \delta_{1,H,r} I_{(r)}(x_{H,j}) \right) \cdot \left[w_t \left(I_{\{a_2\}}(a') + \frac{1}{\gamma} I_{\{a_1\}}(a') \right) \right] + \quad (7c)$$

$$+ \left(\beta_2 + \sum_{r=1}^{n_S} \delta_{2,S,r} I_{(r)}(x_{S,j}) + \sum_{r=1}^{n_T} \delta_{2,T,r} I_{(r)}(x_{T,j}) + \sum_{r=1}^{n_P} \delta_{2,P,r} I_{(r)}(x_{P,j}) + \quad (7d)$$

$$\sum_{r=1}^{n_H} \delta_{2,H,r} I_{(r)}(x_{H,j}) \right) \cdot (w_{t,j} - \psi)^\tau \cdot I_{\{w_{t,j} - \psi > 0\}}(w_{t,j}) \cdot I_{\{a_2\}}(a') + \quad (7e)$$

$$+ u_{t,j} \quad (7f)$$

where deltas referred to the same categorical variable add to zero (sum-to-zero parameterization), e.g. $\sum_{r=1}^{n_S} \delta_{2,S,r} = 0$; exogenous random variables are Normal, $U_{t,j} \sim N(0, \sigma_Y^2)$, $t \in \{1, 2, 3\}$, with constant variance, and they represent the overall contribution of all causal determinants not accounted for as endogenous variables to the electrical resistance Y_t . Variables like surface finish and humidity change the slope of time through parameters like $\delta_{1,S} = (\delta_{1,S,1}, \dots, \delta_{1,S,n_S})$ and $\delta_{1,H} = (\delta_{1,H,1}, \dots, \delta_{1,H,n_H})$ (equation 7, lines 7b and 7c), while parameters like $\delta_{2,S} = (\delta_{2,S,1}, \dots, \delta_{2,S,n_S})$ and $\delta_{2,H} = (\delta_{2,H,1}, \dots, \delta_{2,H,n_H})$ (equation 7, lines 7d and 7e) change the importance of the non-linear component. Parameter ψ defines the location of a knot such that, for W_t smaller than ψ , this non-linear component of time is null (lines 7d and 7e), i.e., if $\psi = 2.0$ this component is equal to zero during the first 2000 hours. The exponent τ controls the amount of non-linear change in the AS regime, $A = a_2$, and $\tau = 3.0$ seems a plausible value in our context.

Last, the regime indicator $A = a_1$ makes the non-linear component null because, without acceleration, the change of electrical resistance is linear in time for all the lifespan of a device. Furthermore, the time transformation function defined in line (7c) of equation (7) is introduced because under the NS regime at time w_t the increase of the electrical resistance is γ times smaller than the increase under the AS regime at the same time w_t . In the following sections, we assume that $\gamma = 10$, therefore 1000 hours in the NS regime are equivalent to 100 hours in the AS regime for the linear-in-time portion of the increase in electrical resistance. This part of the elicitation, where the two regimes are heavily related, depends on the knowledge of the underlying physics of failure. Indeed, the elicited equation is specific for the considered context, but we believe that it may accommodate many other contexts by selecting plausible intervals of parameters in equation (7), like γ, ψ and τ .

The elicited causal DAG suited to observational studies (Figure 3) under the NS regime is also useful for experimental studies in the AS regime after deriving the implied submodel (Pearl, 2009, section 7.1.2). During an experiment, X_S, X_T, X_P, X_H are under full control of the technologist, for example humidity is maintained into a predefined interval of values and the surface finish is assigned by randomization. The edges originated from X_H and reaching nodes X_S, X_T are deleted, and U_H, U_S, U_T, U_P are removed because these nodes do not define values of X_H, X_S, X_T, X_P anymore. If the observation times are assigned and known without uncertainty for each device, then variables W_t , $t > 0$, become known constants and all correspondent U_t are also removed from the DAG. Nodes W_1, W_2, W_3 , as well as nodes X_H, X_S, X_T, X_P , are now represented by squares because they are assigned

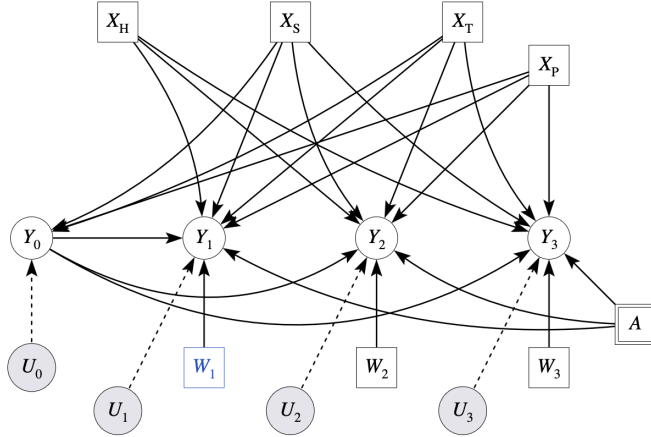


Figure 4: Implied DAG \mathcal{G}_4 representing the submodel exploited to estimate effects of the intervention $do(x_S, x_T, x_P, x_H)$, with $A = a_2$ the regime indicator.

constants. After taking account of the intervention, the DAG in Figure (3) is transformed into the DAG in Figure (4).

5 Causal estimates leveraging two synthetic datasets

A causal estimand is a quantity of interest for the technologist, a key question in the considered context. It may differ according to the stress regime applied to electronic devices besides the specific purpose of the analysis.

In this section, two synthetic datasets \mathcal{D}_{NS} and \mathcal{D}_{AS} respectively of size $n_{NS} = 2048$ and $n_{AS} = 1024$ at each time point are considered. The \mathcal{D}_{AS} dataset is made by 8 observations-devices for each possible configuration of X_S, X_T, X_P and X_H : $8 \times 4 \times 4 \times 4 \times 2 = 1024$ statistical units. The \mathcal{D}_{NS} dataset is obtained using the graphical model as generator of synthetic observations for a selected configuration of model parameters. All data are available for download from a dedicated website (see the Online Supplements section). During the analysis, the expert is certain about parameters $\psi = 2.00$, $\tau = 3$, $\gamma = 10$, and the initial target electrical resistance is set to 1000 [ohms].

All statistical analyses were conducted using R (R Core Team 2024) within the RStudio environment (RStudio Team 2023). Data visualization was carried out using the *ggplot2* package (Wickham 2016), while Bayesian modeling was implemented via the *rstan* interface (Stan Development Team 2024) to the STAN probabilistic programming language (Carpenter et al. 2017); utilities from the *bayetestR* package (Makowski et al. 2019) were employed to process the MCMC simulation output.

5.1 Bayesian initial and final distributions

The likelihood function for observational (NS regime) and experimental (AS regime) data is defined through the conditional probability density functions (pdfs) defined in section (4), then, a prior distribution is specified for the model parameters θ .

The posterior distribution of model parameters is approximated by MCMC simulation using the Stan software (Stan Development Team 2025).

The conditional pdf of endogenous variables given parameters in a PGM is defined according to the elicited DAG, thus the likelihood function of conditionally exchangeable observations is defined as:

$$p(v_{1,1}, v_{2,1}, \dots, v_{n_G,n} \mid \boldsymbol{\theta}) = \prod_{j=1}^n \prod_{i=1}^{n_V} p(v_{i,j} \mid pa_i, \boldsymbol{\theta}) \quad (8)$$

where $pa_i = \{pa_{i,1}, pa_{i,2}, \dots\}$ is the vector of the parent variables of v_i . Notably, square nodes do not contribute to equation (8) because they are known constants, like the regime indicator A .

In the observational context (NS regime), the DAG in Figure (3) is exploited after changing W_1, W_2, W_3 into square nodes (known without uncertainty) and modifying equation (8) accordingly.

Prior distributions of parameters in the pdfs of X_H, X_P, X_S, X_T and Y_0, Y_1, Y_2, Y_3 are defined during the elicitation step. Under the assumption that a Dirichlet family of pdfs is suited to represent the expert's degree of belief about categorical variables, the initial (prior) distributions are defined as:

$$p(\boldsymbol{\pi}_{S,r} \mid x_H = r, \boldsymbol{\lambda}_{S,r}, a_1) = \text{Dirichlet}(\boldsymbol{\lambda}_{S,r}) \quad (9)$$

$$p(\boldsymbol{\pi}_{T,r} \mid x_H = r, \boldsymbol{\lambda}_{T,r}, a_1) = \text{Dirichlet}(\boldsymbol{\lambda}_{T,r}) \quad (10)$$

$$p(\boldsymbol{\pi}_P \mid \boldsymbol{\lambda}_P, a_1) = \text{Dirichlet}(\boldsymbol{\lambda}_P) \quad (11)$$

$$p(\boldsymbol{\pi}_H \mid \boldsymbol{\lambda}_H, a_1) = \text{Dirichlet}(\boldsymbol{\lambda}_H) \quad (12)$$

with $r \in \{1, 2, \dots, n_H\}$ and where n_S, n_T are respectively the number of elements in $\boldsymbol{\lambda}_{S,r}$ and $\boldsymbol{\lambda}_{T,r}$. Standard elicitation methods exist to specify the elements of the lambda vectors in the initial distribution (O'Hagan et al. 2006); however, in this work, all elements are set to one.

The exogenous variable pertaining to a measured electrical resistance Y_t follows a zero-mean Normal distribution with constant variance for $U_t, t > 0$. The prior distribution recommended by Gelman (2006) for the standard deviation of a Normal distribution belongs to the half-Student family, so that the shape is quite flat on the right tail and with its maximum at zero, as described in the following:

$$U_{t,j} \sim N(0, \sigma_{U,t}^2) \quad (13)$$

$$\sigma_{U,t} \sim \frac{\text{Student}(3, 0, 2.5)}{1 - \int_{-\infty}^0 \text{Student}(t) dt} \quad (14)$$

with the elicited scale parameter equal to 2.5 and 3 degrees of freedom.

The initial distribution for each coefficient in the polynomial model for Y_t is defined in the location-scale Student family as follows:

$$\delta_{r,q,b} \sim \text{Student}(3, 0, 25) \quad (15)$$

$$\beta_g \sim \text{Student}(3, 0, 50) \quad (16)$$

with $g \in \{1, 2\}$, $r \in \{1, 2\}$, $q \in \{S, T, P, H\}$ and $b \in \{1, 2, \dots, n_q\}$, like in equation (7). Plausible values of these coefficients belong to the interval $(-50, 50)$.

The initial distribution of parameters in the linear predictor of the initial electrical resistance Y_0 are also in the Student family:

$$\alpha_{q,r} \sim Student(3, 0, 25) \quad (17)$$

$$\mu_0 \sim Student(3, 1000, 1000) \quad (18)$$

with $q \in \{S, P, T\}$ and $r \in \{1, \dots, n_q\}$.

The joint initial distribution of model parameters is defined as:

$$p(\boldsymbol{\theta} \mid a_1, \xi) = p(\boldsymbol{\pi}_P \mid \boldsymbol{\lambda}_P) \cdot p(\boldsymbol{\pi}_H \mid \boldsymbol{\lambda}_H) \cdot p(\boldsymbol{\alpha}) \cdot p(\boldsymbol{\sigma}) \cdot p(\boldsymbol{\delta}) \cdot p(\boldsymbol{\beta}) \cdot \prod_r p(\boldsymbol{\pi}_{S,r} \mid x_H = r, \boldsymbol{\lambda}_{S,r}) \cdot \prod_r p(\boldsymbol{\pi}_{T,r} \mid x_H = r, \boldsymbol{\lambda}_{T,r}) \quad (19)$$

where priors for each vector of parameters have been already defined. Unless otherwise specified, (vectors of) parameters are marginally independent.

In an experimental study under the AS regime, $A = a_2$, randomized treatment assignment defines which levels x'_S, x'_T, x'_P of the experimental factors are assigned to a (random) sample of devices. It follows that data in \mathcal{D}_{AS} provide information about variables Y_0, Y_1, Y_2, Y_3 . Equation (8) is instantiated accordingly and the prior distribution in this context is limited to:

$$p(\boldsymbol{\theta} \mid a_2, \xi) = p(\boldsymbol{\alpha}) \cdot p(\boldsymbol{\sigma}) \cdot p(\boldsymbol{\delta}) \cdot p(\boldsymbol{\beta}) \quad (20)$$

as can be appreciated in DAG (4), after considering the implied likelihood function.

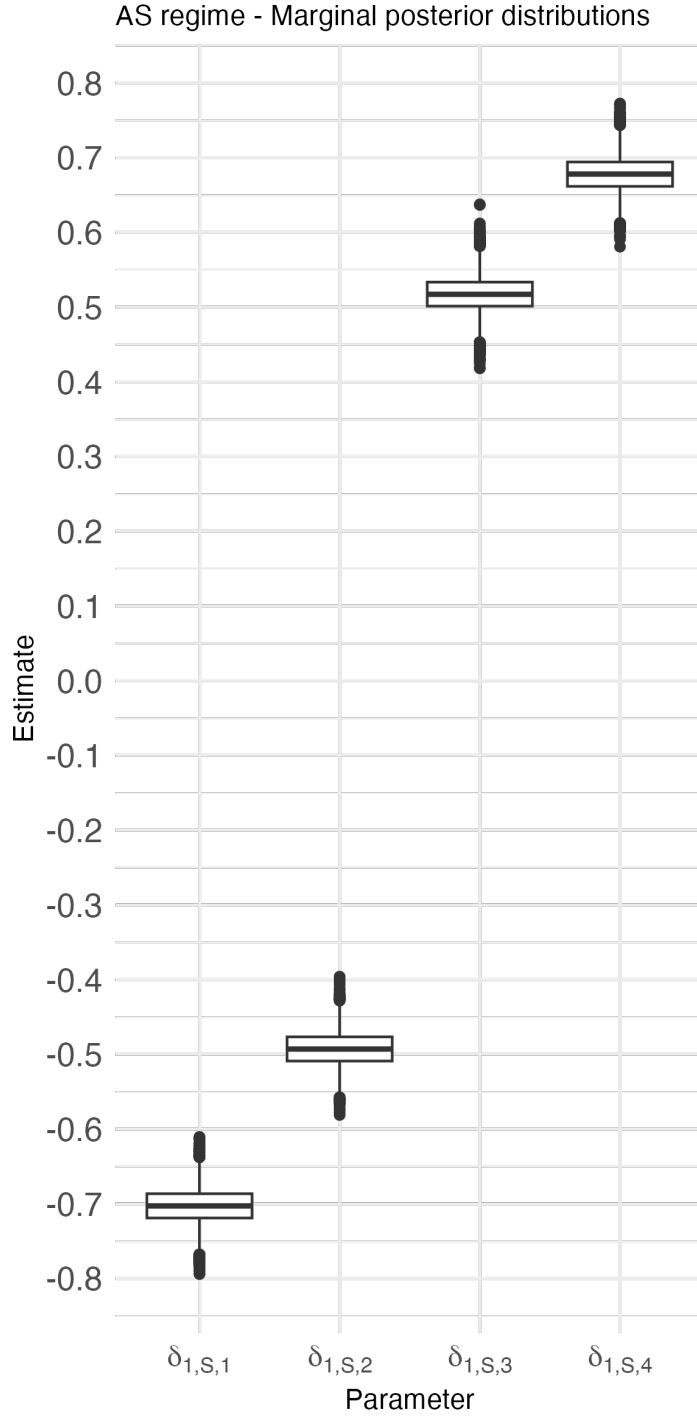
Bayesian model fitting is performed at first by running a MCMC simulation for \mathcal{D}_{AS} using the initial pdf (20), and then for \mathcal{D}_{NS} using as prior distribution equation (19). Table 1 summarizes the results about model parameters in equation (7) under both the AS and NS regimes (i.e., posterior estimates, posterior standard deviation, and 95% Highest Posterior Density Intervals). For the sake of brevity, we consider the surface finish coefficients $\delta_{1,S,1}$, $\delta_{1,S,2}$, $\delta_{1,S,3}$, and $\delta_{1,S,4}$. Under both the AS and the NS regimes, the corresponding posterior estimates are very close to the true parameter values, with very low posterior standard deviations. Satisfactory results are also obtained for the remaining coefficients in equation (7).

Table 1: Summary of model (7), surface finish parameters: posterior estimates, posterior standard deviation, 95% Highest Density Interval-HDI.

Regime	Symbol	True value	Post. estimate	Post. Std. Dev.	95% HDI
AS					
	$\delta_{1,S,1}$	-0.700	-0.702	0.024	[-0.750, -0.660]
	$\delta_{1,S,2}$	-0.500	-0.493	0.024	[-0.540, -0.450]
	$\delta_{1,S,3}$	0.500	0.517	0.024	[0.470, 0.570]
	$\delta_{1,S,4}$	0.700	0.678	0.024	[0.630, 0.720]
NS					
	$\delta_{1,S,1}$	-0.700	-0.682	0.021	[-0.720, -0.640]
	$\delta_{1,S,2}$	-0.500	-0.497	0.014	[-0.530, -0.470]
	$\delta_{1,S,3}$	0.500	0.510	0.016	[0.480, 0.540]
	$\delta_{1,S,4}$	0.700	0.669	0.016	[0.640, 0.700]

Figure (5) reports the box-plots of the posterior estimates for the surface-finish parameters under the AS regime. The posterior medians are very close to the true parameter values, with very narrow interquartile ranges, confirming the accuracy of the posterior estimates.

Figure 5: Boxplot of the marginal posterior distributions for parameters $\delta_{1,S,1}, \delta_{1,S,2}, \delta_{1,S,3}, \delta_{1,S,4}$ under the AS regime.



5.2 The increase of electrical resistance in the AS regime

The first estimand quantifies the expected increase of electrical resistance after w_t hours of work for electronic devices configured as x'_S, x'_T, x'_P after operating under humidity x'_H :

$$\Delta_1(x'_S, x'_T, x'_P, x'_H, w_t, a_2) = E[Y_t - Y_0 \mid do(x'_S, x'_T, x'_P, x'_H, w_t), a_2] = \quad (21a)$$

$$= E[Y_t \mid x'_S, x'_T, x'_P, x'_H, w_t, a_2] - E[Y_0 \mid x'_S, x'_T, x'_P, w_t, a_2] = \quad (21b)$$

$$= (\beta_1 + \delta_{1,S,[x'_S]} + \delta_{1,T,[x'_T]} + \delta_{1,P,[x'_P]} + \delta_{1,H,[x'_H]}) \cdot w_t + \quad (21c)$$

$$+ (\beta_2 + \delta_{2,S,[x'_S]} + \delta_{2,T,[x'_T]} + \delta_{2,P,[x'_P]} + \delta_{2,H,[x'_H]}) \cdot (w_t - \psi)^\tau \cdot I_{\{w_t - \psi > 0\}}(w_t)$$

where $\delta_{1,S,[x'_S]}$ is the parameter corresponding to surface finish $X_S = x'_S$ and where a corresponding notation holds for all other deltas; typical times of measurement are $w_t \in \{0.00, 0.72, 2.16, 3.60\}$ kilohours.

In Table 2 we report an example with the values for the estimand (21), calculated for two different configurations of (X_S, X_T, X_P, X_H) , i.e., $(1, 1, 1, 1)$ and $(2, 1, 1, 1)$. We evaluate the estimand defined in equation (21) under both configurations, across the following values of w_t : $\{0.72, 1.50, 2.00, 2.16, 2.50, 3.00, 3.60\}$. The posterior standard deviations for all coefficients are low, and the 95% Highest Posterior Density Intervals are narrow, further confirming the accuracy of the parameter estimates in model (7).

Table 2: Estimand (21) with two configurations. Time is expressed in units of 10^3 hours (kilohours).

Configuration (X_S, X_T, X_P, X_H)	Time w_t	Estimate	Std. Dev	95% HDI
{1, 1, 1, 1}	0.72	7.330	0.039	[7.260, 7.410]
	1.50	15.270	0.080	[15.120, 15.430]
	2.00	20.360	0.107	[20.150, 20.570]
	2.16	22.116	0.116	[21.890, 22.350]
	2.50	29.324	0.129	[29.080, 29.580]
	3.00	61.530	0.123	[61.290, 61.770]
	3.60	163.581	0.116	[163.350, 163.810]
{2, 1, 1, 1}	0.72	7.481	0.038	[7.400, 7.550]
	1.50	15.585	0.080	[15.420, 15.740]
	2.00	20.781	0.107	[20.560, 20.990]
	2.16	22.611	0.115	[22.380, 22.830]
	2.50	31.101	0.129	[30.840, 31.340]
	3.00	72.170	0.123	[71.930, 72.410]
	3.60	205.337	0.116	[205.110, 205.570]

5.3 Increase in electrical resistance under the AS regime with varying configurations

The expected increment of electrical resistance Δ_1 may change according to alternative configurations of the electronic devices, like levels $x'_S \neq x''_S$, and in general for different levels of type, $x'_T \neq x''_T$ and pins, $x'_P \neq x''_P$. The most general contrast of expected increments is a function of two different tuples of levels (x'_S, x'_T, x'_P) and (x''_S, x''_T, x''_P) for the experimental factors, while keeping humidity x_H , time w_t and stress regime a_2 at constant values, as described below:

$$\Delta_{S,T,P}(x'_S, x'_T, x'_P, x''_S, x''_T, x''_P, x_H, w_t, a_2) = \quad (22a)$$

$$= \Delta_1(x''_S, x''_T, x''_P, x_H, w_t, a_2) - \Delta_1(x'_S, x'_T, x'_P, x_H, w_t, a_2) = \quad (22b)$$

$$= \left[\sum_{q \in \{S,T,P\}} \sum_{i=1}^{n_q} \delta_{1,q,i} (I_{(i)}(x''_q) - I_{(i)}(x'_q)) \right] w_t + \quad (22c)$$

$$+ \left[\sum_{q \in \{S,T,P\}} \sum_{i=1}^{n_q} \delta_{2,q,i} (I_{(i)}(x''_q) - I_{(i)}(x'_q)) \right] \cdot (w_t - \psi)^\tau \cdot I_{\{w_t - \psi > 0\}}(w_t)$$

where the sum over index q covers all the experimental factors.

The estimand in (22a) includes all instances of contrast in which just one experimental factor at a time varies. If only X_S takes two different values x'_S and x''_S , the estimand becomes:

$$\begin{aligned} \Delta_S(x'_S, x''_S, x_H, w_t, a_2) &= \Delta_{S,T,P}(x'_S, x_T, x_P, x''_S, x_T, x_P, x_H, w_t, a_2) = \\ &= (\delta_{1,S,[x'_S]} - \delta_{1,S,[x''_S]}) \cdot w_t + (\delta_{2,S,[x'_S]} - \delta_{2,S,[x''_S]}) \cdot (w_t - \psi)^\tau \cdot I_{\{w_t - \psi > 0\}}(w_t) \end{aligned} \quad (23)$$

where, $\delta_{2,S,[x''_S]}$ is the value to consider for $X_S = x''_S$. In equation (23), Δ_S is a shortcut notation highlighting the experimental factor varied. Similar causal estimands $\Delta_T(x'_T, x''_T, x_H, w_t, a_2)$ and $\Delta_P(x'_P, x''_P, x_H, w_t, a_2)$ are defined for the other two experimental factors.

Table 3 reports the values of estimand (23), computed using the same set of w_t values as in equation (21). Estimand (23) represents the one-factor contrast for the two different surface finish values considered when calculating estimand (21) in Table 2. The low standard deviations and narrow 95% HPD intervals confirm that the obtained results are satisfactory.

Table 3: Estimand (22): one-factor contrasts for two different values of surface finish

Estimand	Estimate	Std. Dev.	95% HDI
$\Delta_S(x'_S, x''_S, x_H, w_t, a_2)$			
$\Delta_S(1, 2, 1, 0.72, a_2)$	0.151	0.028	[0.100, 0.210]
$\Delta_S(1, 2, 1, 1.50, a_2)$	0.315	0.059	[0.200, 0.430]
$\Delta_S(1, 2, 1, 2.00, a_2)$	0.420	0.078	[0.270, 0.570]
$\Delta_S(1, 2, 1, 2.16, a_2)$	0.495	0.084	[0.330, 0.660]
$\Delta_S(1, 2, 1, 2.50, a_2)$	1.777	0.094	[1.590, 1.960]
$\Delta_S(1, 2, 1, 3.00, a_2)$	10.640	0.086	[10.470, 10.810]
$\Delta_S(1, 2, 1, 3.60, a_2)$	41.756	0.090	[41.580, 41.940]

5.4 Reliability of a future device in the AS regime

A causal effect on reliability (failure time) is defined by the change in reliability (survival) times under different treatment conditions, for example a difference in median reliability (survival) time between treated and untreated groups. The failure time T depends on the difference of initial, $Y_{0,j}$ and final, $Y_{t,j}$, values of electrical resistance, but also on the threshold described as 10% of $Y_{0,j}$, a quantity specific for observation (device) j .

We now consider a future device that could be added to increase the sample size to $n + 1$, and we maintain index j to refer to this new statistical unit. At the beginning of the study, just after the device is measured, the random variable to consider is as follows:

$$D_{0,j} = Y_{t,j} - 1.1 \cdot y_{0,j} \quad (24)$$

which is a member of the Normal family of pdfs, thus from equation (7) we have:

$$p(d_{0,j} \mid y_{0,j}, do(x_S, x_T, x_P, x_H, w_t), a_2) = N(d_{0,j} \mid \mu_{D,0,j}, \sigma_Y^2) \quad (25)$$

where parameter σ_Y^2 is the variance of the exogenous variable $U_{t,j}$, while $\mu_{D,0,j}$ is equal to

the linear predictor r.h.s. of equation (7), lines (7b-7e), after simplification:

$$\mu_{D,0,j}(w_{t,j}) = h_D(\mathbf{x}, w_{t,j}, \boldsymbol{\theta}) - 0.1 \cdot y_{0,j} = \quad (26a)$$

$$= \left(\beta_1 + \sum_{r=1}^{n_S} \delta_{1,S,r} I_{(r)}(x_{S,j}) + \sum_{r=1}^{n_T} \delta_{1,T,r} I_{(r)}(x_{T,j}) + \sum_{r=1}^{n_P} \delta_{1,P,r} I_{(r)}(x_{P,j}) + \right. \quad (26b)$$

$$\left. + \sum_{r=1}^{n_H} \delta_{1,H,r} I_{(r)}(x_{H,j}) \right) \cdot \left[w_t \left(I_{\{a_2\}}(A) + \frac{1}{\gamma} I_{\{a_1\}}(A) \right) \right] + \quad (26c)$$

$$+ \left(\beta_2 + \sum_{r=1}^{n_S} \delta_{2,S,r} I_{(r)}(x_{S,j}) + \sum_{r=1}^{n_T} \delta_{2,T,r} I_{(r)}(x_{T,j}) + \sum_{r=1}^{n_P} \delta_{2,P,r} I_{(r)}(x_{P,j}) + \right. \quad (26d)$$

$$\left. \sum_{r=1}^{n_H} \delta_{2,H,r} I_{(r)}(x_{H,j}) \right) \cdot (w_{t,j} - \psi)^\tau \cdot I_{\{w_{t,j} - \psi > 0\}}(w_{t,j}) \cdot I_{\{a_2\}}(A) + \quad (26e)$$

$$- 0.1 \cdot y_{0,j}. \quad (26f)$$

with the notation $\mu_{D,0,j}(w_{t,j})$ emphasizing the dependence of the expected value on time $w_{t,j}$. The reliability function for device j introduced in equation (1) is rewritten in terms of change of electrical resistance, conditional of the observed time t_j , as follows:

$$R(t_j | y_{0,t}, a_2, do(\mathbf{x}), \boldsymbol{\theta}) = P[D_{0,j} < 0 | W_{t,j} = t_j, y_{0,j}, a_2, do(\mathbf{x}), \boldsymbol{\theta}] = \quad (27a)$$

$$= \int_{-\infty}^0 N(q | \mu_{D,0,j}(t_j), \sigma_Y^2) dq \quad (27b)$$

with $do(\mathbf{x}) = do(x_S, x_T, x_P, x_H)$; to avoid ambiguity, we use q as the variable of integration instead of $d_{0,j}$. If the vector $\boldsymbol{\theta}$ of model parameters is known in equation (27a), as well as the considered factors, then the reliability is just a function of time t_j (equation 27b).

The above analysis is now extended to a future device, again indexed as j , which belongs to the group of devices with configuration \mathbf{x} , the only known information about it. The difference $D_j = Y_j - 1.1 \cdot Y_{0,j}$ conditional on time w_t , after simplification, is a random variable with expected value $\mu_D(w_t)$:

$$\mu_D(w_t) = E[h_D(\mathbf{x}, w_t, a_2, \boldsymbol{\theta}) + U_{t,j} - 0.1 \cdot Y_{0,j}] = \quad (28a)$$

$$= h_D(\mathbf{x}, w_t, a_2, \boldsymbol{\theta}) + E[U_{t,j}] - 0.1 h_0(\mathbf{x}, w_t, \boldsymbol{\theta}) - 0.1 E[U_{0,j}] = \quad (28b)$$

$$= h_D(\mathbf{x}, w_t, a_2, \boldsymbol{\theta}) - 0.1 h_0(\mathbf{x}, w_t, \boldsymbol{\theta}) \quad (28c)$$

since $h_D(\mathbf{x}, w_t, a_2, \boldsymbol{\theta})$ does not vary, as well as the linear predictor $h_0(\mathbf{x}, w_t, \boldsymbol{\theta})$, and $E[U_{0,j}] = E[U_{t,j}] = 0$. The variance of this difference becomes:

$$\sigma_D^2 = Var[D_j] = Var[Y_{t,j} - 1.1 Y_{0,j}] = \quad (29a)$$

$$= Var[h_D(\mathbf{x}, w_t, a_2, \boldsymbol{\theta}) + U_{t,j} - 0.1 h_0(\mathbf{x}, w_t, \boldsymbol{\theta}) - 0.1 U_{0,j}] \quad (29b)$$

$$= Var[U_{t,j} - 0.1 U_{0,j}] = \sigma_Y^2 + 0.01 \sigma_0^2 \quad (29c)$$

since the variance of constants is null and exogenous variables are not correlated; given the normality of exogenous variables, the distribution of this difference is Normal, $D_j \sim N(\mu_D(w_t), \sigma_D^2)$. We conclude that in this context, the reliability function is:

$$R(t_j | a_2, do(\mathbf{x}), \boldsymbol{\theta}) = P[D_j < 0 | W_{t,j} = t_j, a_2, do(\mathbf{x}), \boldsymbol{\theta}] = \quad (30a)$$

$$= \int_{-\infty}^0 N(q | \mu_D(t_j), \sigma_D^2) dq \quad (30b)$$

with $\mu_D(t_j)$ and σ_D^2 defined above; for notational convenience, q is used in place of d_j within the integral.

Figure (6) shows the estimated reliability functions related to formulas (27) and (30), with unknown (bottom) and known (top) Y_0 , respectively. Both functions are calculated under the configuration $(X_S, X_T, X_P, X_H) = (1, 1, 1, 1)$.

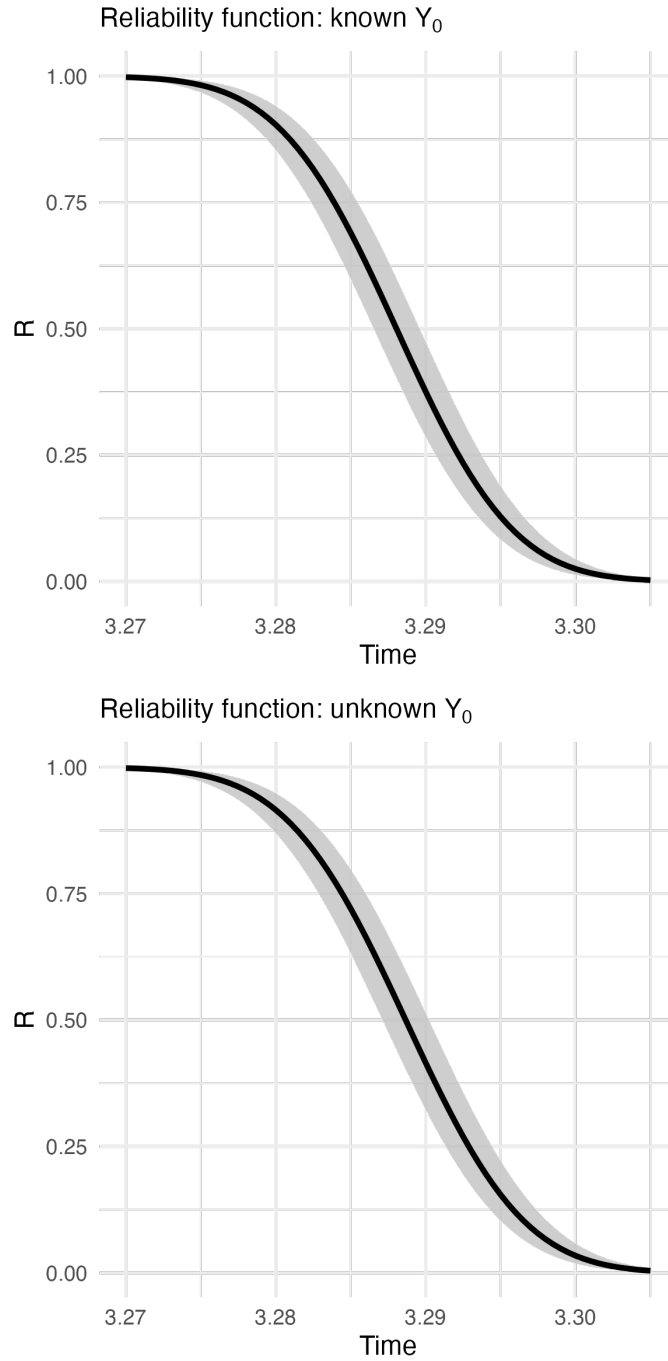


Figure 6: Estimated reliability functions with unknown Y_0 (bottom), equation (27), and known Y_0 (top), equation (30).

5.5 Observational studies in the NS regime

Estimates of the causal effects of X_S and X_T on Y_t are biased when based on observational data in the NS regime ($A = a_1$), due to the presence of the confounder X_H . Conditioning on X_H suffices to eliminate confounding bias, as stated by Pearl’s back-door criterion (Pearl 2009, sec. 3.3.1). The truncated product formula is defined here by removing all conditional pdfs associated with the selected intervention and by marginalizing over the confounder (Pearl 2009, sec. 3.2.3 and note 4 page 72). The resulting expression is as follows:

$$\begin{aligned} p(y_t, y_0 \mid do(x_S, x_T, x_P), w_t, a_1) &= \\ &= p(y_0 \mid x_S, x_T, x_P) \sum_{x_H} p(y_t \mid x_S, x_T, x_P, x_H, y_0, w_t, a_1) p(x_H) \end{aligned} \quad (31)$$

where $do(x_S, x_T, x_P)$ represents the intervention of interest. Nevertheless, the failure time W_f of a device is a function of Y_t, Y_0, w_t, θ , thus the distribution of the failure time W_f is derived given a selected intervention, assuming all model parameters are known, i.e., conditional on θ . The Bayesian predictive distribution of failure time W_f accounts for the uncertainty about model parameters and is conditional on a given surface, type and pin. A MCMC sample of draws from the predictive distribution of failure time W_f is exploited to estimate the main features of this distribution. To illustrate the approach, we consider the intervention $do(x_S = 1, x_T = 1, x_P = 4)$: for each parameter value $\theta^{(i)}$ sampled from the posterior distribution at iteration (i) , we draw a realization from the predictive distribution of $p(x_H \mid \theta)$, then we draw a realization from the corresponding component of the mixture distribution. The same algorithm is followed for the intervention $do(x_S = 3, x_T = 3, x_P = 3)$. After obtaining the two histograms (Figure 7), a Normal pdf is fitted for each intervention, and displayed as an overlapped continuous line. Small departures from normality are present in both histograms. In Table (4), summaries of W_f for the two considered interventions are shown, and is clear the huge differences of the two failure time distributions in the considered population. The credible interval of level 0.90 for the first intervention is (60.322, 60.913) while for the second one is (54.440, 54.860). Therefore, the two intervals do not overlap: the left endpoint of the first interval differs by more than 5,000 hours from the right endpoint of the second one. Causal estimands based on contrasts of mean values or ratio of variances under different interventions may be derived and evaluated using the MCMC simulation output.

Interval-censored and right-censored observations of failure time characterize our context in the NS regime. If we consider an observation j for which the electrical resistance is $y_{3,j} > 1.1 y_{0,j}$ at time $w_{3,j}$, then we can state that $w_f \in (w_{2,j}, w_{3,j})$, an interval that may span thousands of hours. If the measured electrical resistance $y_{3,j}$ at the latest time point $w_{3,j}$ is less than $1.1 y_{0,j}$, then we can conclude that $w_f > w_{3,j}$.

A natural question is: at what time the equality $y_{3,j} = 1.1 y_{0,j}$ holds for device j ? We rephrase this question in counterfactual terms: given that the electrical resistance is measured at time $w_{3,j}$ and the corresponding observed value is $y_{3,j} \neq 1.1 y_{0,j}$, what time could have been selected instead to obtain $y_{3,j} = 1.1 y_{0,j}$ under the same assembly configuration and humidity conditions?

In Pearl’s twin-network approach (Pearl 2009, section 7.1.4), it is possible to obtain counterfactual quantities by setting the value of some selected variables (Figure 2, section 3) to whatever value is of interest. Then, the failure time $W_{f,j}$ for device j may be inferred as a counterfactual quantity: it is the time t at which the electrical resistance $y_{t,j}$ of an electronic device j would have reached $1.1 y_{0,j}$ had the observation time w_t been equal to

Table 4: Summary statistics (kilohours) about the estimated distribution of the failure time under the NS regime with intervention (a): $do(x_S = 1, x_T = 1, x_P = 4)$, and (b): $do(x_S = 3, x_T = 3, x_P = 3)$.

Statistic	(a): $do(x_S = 1, x_T = 1, x_P = 4)$	(b): $do(x_S = 3, x_T = 3, x_P = 3)$
Min.	59.938	54.124
$w_{f,0.05}$	60.322	54.440
$w_{f,0.25}$	60.496	54.564
$w_{f,0.50}$	60.618	54.648
$w_{f,0.75}$	60.741	54.736
$w_{f,0.95}$	60.913	54.860
Max.	61.398	55.206
Mean	60.618	54.650
Std. Dev.	0.180	0.127

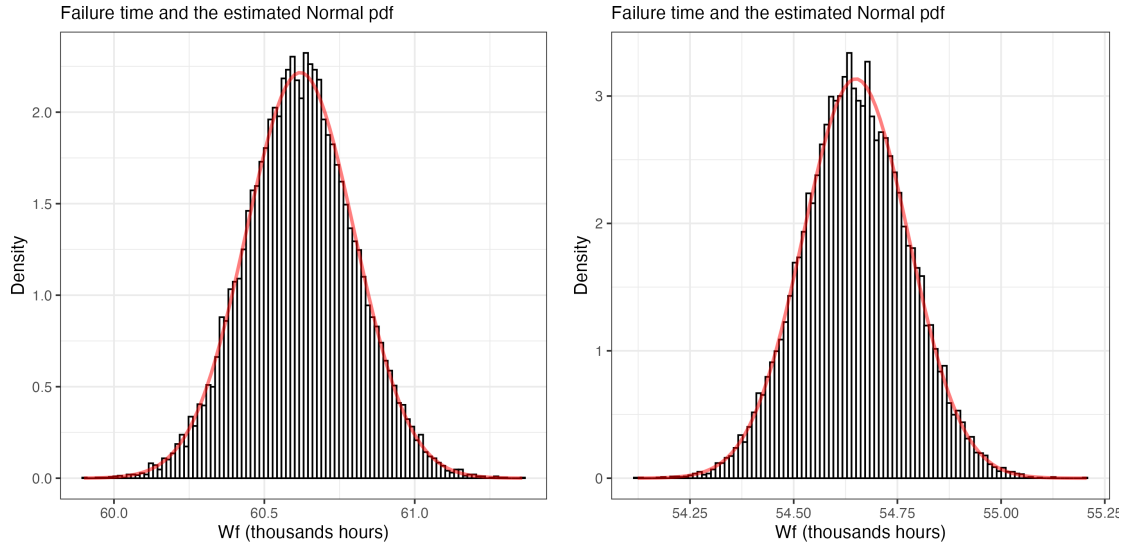


Figure 7: Estimated pdf of W_f in kilohours, given the intervention $do(x_S = 1, x_T = 1, x_P = 4)$, left, and under $do(x_S = 3, x_T = 3, x_P = 3)$, right.

the solution of the equation:

$$0.1 \cdot y_{0,j} - \left(\beta_1 + \sum_{r=1}^{n_S} \delta_{1,S,r} I_{(r)}(x_{S,j}) + \sum_{r=1}^{n_T} \delta_{1,T,r} I_{(r)}(x_{P,j}) + \sum_{r=1}^{n_P} \delta_{1,P,r} I_{(r)}(x_{T,j}) + \sum_{r=1}^{n_H} \delta_{1,H,r} I_{(r)}(x_{H,j}) \right) \cdot \frac{w_t}{\gamma} - u_{3,j} = 0 \quad (32)$$

in the observational regime, $A = a_1$, thus:

$$w_{f,j} \mid \boldsymbol{\theta} = \frac{0.1 \cdot y_{0,j} - u_{3,j}}{\beta_1 + \delta_{1,S,[j]} + \delta_{1,T,[j]} + \delta_{1,P,[j]} + \delta_{1,H,[j]}} \cdot \gamma \quad (33)$$

which is a quantity whose distribution, conditional on the factual observations $y_{0,j}, y_{t,j}$, is governed by the posterior distribution $p(\boldsymbol{\theta} \mid \mathcal{D})$ of model parameters. It is worth noting that equation (33) does not contain $y_{t,j}$; nevertheless, this value is needed to compute the realized residual $u_{t,j} \mid \boldsymbol{\theta}^{(g)}$ using equation (7), where $\boldsymbol{\theta}^{(g)}$ denotes the value of the parameter vector sampled at iteration $g = 1, 2, \dots, G$ in the MCMC simulation. Similarly, the coefficients in the denominator are elements in $\boldsymbol{\theta}^{(g)}$. An MCMC sample to approximate the final distribution of the counterfactual variable $W_{f,j}$ is obtained by iterating the following steps: i) compute the residual $u_{3,j}$ given the current value $\boldsymbol{\theta}^{(g)}$ and the observed values $y_{t,j}, y_{0,j}$; ii) calculate $w_{f,j}$ in equation (33) by replacing model parameters and the implied residual; iii) iterate the above steps for G times, the sample size of the MCMC simulation after warmup.

To illustrate the approach, we consider device ID2436, which showed $Y_{0,j} = 1003$ and $Y_{3,j} = 1070$ ohms at $w_{3,j} = 36$ kilohours. The distribution of the counterfactual failure time $W_{f,j}$, approximated by MCMC, has mean and median of 53.690 kilohours, standard deviation of 0.0185 kilohours and 5th and 95th percentiles given by $w_{f,j,0.05} = 53.660$ and $w_{f,j,0.95} = 53.720$, respectively. In other words, in a context where hourly measurements are performed, the failure time could have been observed at $\widehat{E}[W_{f,j}] = 53690$ hours, i.e., approximately six years of operation.

Counterfactuals are also useful in an hypothetical context of a lawsuit filed by a client against the manufacturer of device j . The contract signed by the parties stipulates that at 21.6 kilohours, the electrical resistance of device j is almost certainly less than or equal to 1040 ohms. However, the client claims to have measured a value of 1041.056 ohms. The manufacturer defends itself by pointing out that the contract also specified a normal humidity level during operations, whereas during company inspections at the client's site, the humidity was consistently found to be high. What would the measured electrical resistance have been at time 21.6 kilohours, had the humidity level been kept normal, whereas it was actually kept high and we measured $Y_{2,j} = 1041.056$ ohms?

The answer follows the aforementioned algorithm, except that step (ii) is replaced by the calculation of the counterfactual value $Y_{2,j,x_H}(-1)$, conditional on $\boldsymbol{\theta}^{(g)}$. This value is defined as the sum of $y_{0,j}$, the estimated residual $u_{2,j}^{(g)}$, and the linear predictor including all previously estimated coefficients, except for the one associated with humidity, since the factual value $x_H = 1$ is replaced by the counterfactual value $x_H = -1$. The sample of $G = 20,000$ counterfactual values for $Y_{2,j,x_H}(-1)$ are all less than or equal to 1034.869 ohms, and the credible interval of size 0.98 has endpoints (1034.507, 1034.759). What claimed by the manufacturer is well supported by the estimated distribution of $Y_{2,j,x_H}(-1)$. We note in passing that in a legal context, 'almost sure' might correspond to a probability value smaller than 1×10^{-5} .

6 Final remarks and conclusions

In this paper, a parametric SCM for electrical resistance is proposed to study the effects of three experimental factors, using data collected on electronic devices operating under either an accelerated stress regime or a no-stress regime. We believe that our proposal represents the simplest non-trivial context from which several extensions are possible. This is the reason why a comprehensive summary addressing all recent and ongoing methodological research is not provided here. For example, Correa & Bareinboim (2024) generalize Pearl’s do-calculus from interventional to counterfactual reasoning and introduce a new graphical representation called Ancestral Multi-World Network. Nevertheless, we consider only the factual world and a single counterfactual world in our context.

Model extensions are required when different batches of devices are manufactured in separate production facilities, since transportability must be considered in the analysis (Bareinboim & Pearl 2016). This is also relevant if both sources of information, $\mathcal{D}_{AS,NS}$, are available for the considered class of electronic devices. Transferability makes it possible to learn about correspondent model parameters across different regimes or sources.

Future work might consider more structured contexts, where interaction terms between investigated factors are needed. The location parameter ψ and the exponent τ might be affected by epistemic uncertainty, therefore additional observation times should be planned to contain the resulting uncertainty. In our case study, the observation time for each electronic device was also treated as known without uncertainty, but in other contexts, deviations from the nominal observation value might be of critical importance, e.g., very small σ_0^2, σ_Y^2 and large deltas.

Similar considerations apply to the marginal independence of the exogenous random variables $\{(u_{0,1}, \dots, u_{0,n}, \dots, u_{t,1}, \dots, u_{t,n}) : t = 1, 2, 3\}$. According to our expert, this assumption is reasonable in the context presented here. However, it may not hold in more structured settings unless the model is appropriately extended. In many contexts, model granularity is the key factor that determines the extent to which the specified model approximates the true data-generating process.

Funding

The authors gratefully acknowledge the financial support from the Italian Ministry of University and Research (MUR) under the Project of Relevant National Interest (PRIN 2022), project code E3DM - Experimental Design and Maintenance, a Decision-Making approach driven by Degradation Models - CUP master: B53C24006390006, CUP: B53C24006400006.



Online supplements

The project repository *rel4dev* is currently under development, and the two datasets can be downloaded from it: <https://github.com/federico-m-stefanini/rel4dev>

References

- Bareinboim, E., Correa, J. D., Ibeling, D. & Icard, T. (2022), On pearl’s hierarchy and the foundations of causal inference, *in* H. Geffner, R. Dechter & J. Y. Halpern, eds, ‘Probabilistic and Causal Inference - The Works of Judea Pearl’, Association for Computing Machinery, New York, pp. 507–556.
URL: <https://doi.org/10.1145/3501714.3501743>
- Bareinboim, E. & Pearl, J. (2016), ‘Causal inference and the datafusion problem’, *Proceedings of the National Academy of Sciences* **113**(27), 7345–7352.
URL: <https://doi.org/10.1073/pnas.1510507113>
- Berzuini, C., Dawid, P. & Bernardinelli, L. (2012), *Causality. Statistical perspectives and applications*, John Wiley & Sons, Cambridge, UK.
URL: <https://doi.org/10.1002/9781119945710>
- Brand, J. E., Zhou, X. & Xie, Y. (2023), ‘Recent developments in causal inference and machine learning’, *Annual Review of Sociology* **49**, 81–110.
URL: <https://doi.org/10.1146/annurev-soc-030420-015345>
- Carpenter, B., Gelman, A., Hoffman, M. D., Lee, D., Goodrich, B., Betancourt, M., Brubaker, M., Guo, J., Li, P. & Riddell, A. (2017), ‘Stan: A probabilistic programming language’, *Journal of Statistical Software* **76**(1), 1–32.
URL: <https://doi.org/10.18637/jss.v076.i01>
- Correa, J. & Bareinboim, E. (2024), Counterfactual graphical models: Constraints and inference, Technical Report R-115, Causal Artificial Intelligence Lab, Columbia University.
URL: <https://causalai.net/r115.pdf>
- Degtiar, I. & Rose, S. (2023), ‘A review of generalizability and transportability’, *Annual Review of Statistics and Its Application* **10**, 501–524.
URL: <https://doi.org/10.1146/annurev-statistics-042522-103837>
- Dominici, F., Bargagli-Stoffi, F. J. & Mealli, F. (2021), ‘From controlled to undisciplined data: Estimating causal effects in the era of data science using a potential outcome framework’, *Harvard Data Science Review* **3**(3), 1–34.
URL: <https://doi.org/10.1162/99608f92.8102afed>
- Gelman, A. (2006), ‘Prior distributions for variance parameters in hierarchical models (comment on article by browne and draper)’, *Bayesian Analysis* **1**(3), 515–534.
URL: <https://doi.org/10.1214/06-BA117A>
- Hund, L. & Schroeder, B. (2020), ‘A causal perspective on reliability assessment’, *Reliability Engineering & System Safety* **195**, 106678.
URL: <https://doi.org/10.1016/j.res.2019.106678>
- Makowski, D., Ben-Shachar, M. & Lüdtke, D. (2019), ‘bayestestr: Describing effects and their uncertainty, existence and significance within the bayesian framework’, *Journal of Open Source Software* **4**, 1541.
URL: <https://doi.org/10.21105/joss.01541>
- Meeker, W. Q., Escobar, L. A. & Pascual, F. J. (2021), *Statistical Methods for Reliability Data*, 2 edn, Wiley, Hoboken, NJ.

- O'Hagan, A., Buck, C. E., Daneshkhah, A., Eiser, J. R., Garthwaite, P. H., Jenkinson, D. J., Oakley, J. E. & Rakow, T. (2006), *Uncertain Judgements: Eliciting Experts' Probabilities*, John Wiley & Sons, Chichester.
- Pearl, J. (2009), *Causality: Models, Reasoning and Inference*, 2 edn, Cambridge University Press, Cambridge.
URL: <https://doi.org/10.1017/CBO9780511803161>
- R Core Team (2024), *R: A Language and Environment for Statistical Computing*, R Foundation for Statistical Computing, Vienna, Austria.
URL: <https://www.R-project.org/>
- RStudio Team (2023), *RStudio: Integrated Development Environment for R*, Posit Software, PBC, Boston, MA.
URL: <https://www.posit.co/>
- Ruiz-Tagle, A., Lopez-Droguett, E. & Groth, K. M. (2022), 'A novel probabilistic approach to counterfactual reasoning in system safety', *Reliability Engineering & System Safety* **228**, 108785.
URL: <https://doi.org/10.1016/j.res.2022.108785>
- Singpurwalla, N. D. (2006), *Reliability and Risk: A Bayesian Perspective*, John Wiley & Sons, Chichester.
URL: <https://doi.org/10.1002/9780470060346>
- Stan Development Team (2024), 'Rstan: the r interface to stan', <https://mc-stan.org/>. R package version 2.32.3.
- Stan Development Team (2025), *Stan Modeling Language Users Guide and Reference Manual, Version 2.36*.
URL: <https://mc-stan.org>
- Vonk, M. C., Malekovic, N., Bäck, T. & Kononova, A. V. (2023), 'Disentangling causality: Assumptions in causal discovery and inference', *Artificial Intelligence Review* **56**, 10613–10649.
URL: <https://doi.org/10.1007/s10462-023-10411-9>
- Wickham, H. (2016), *ggplot2: Elegant Graphics for Data Analysis*, Springer-Verlag, New York.